

---

# Antimicrobial Peptide $^{99m}\text{Tc}$ -Ubiquicidin 29–41 as Human Infection-Imaging Agent: Clinical Trial

Muhammad Saeed Akhtar, MBBS, MSc<sup>1</sup>; Aitzaz Qaisar, MBBS, MSc<sup>1</sup>; Javaid Irfanullah, MBBS, MSc<sup>1</sup>; Javaid Iqbal, MBBS, MSc<sup>1</sup>; Bashir Khan, MSc<sup>2</sup>; Mustansar Jehangir, PhD<sup>2</sup>; Muhammad Afzal Nadeem, MPhil<sup>1</sup>; Muhammad Aleem Khan, MBBS, MSc<sup>1</sup>; Muhammad Shahzad Afzal, MBBS, MSc<sup>1</sup>; Ikram ul-Haq, MBBS, MPhil<sup>3</sup>; and Muhammad Babar Imran, MBBS, PhD<sup>1</sup>

<sup>1</sup>Punjab Institute of Nuclear Medicine, Faisalabad, Pakistan; <sup>2</sup>Isotope Production Division, Pakistan Institute of Nuclear Science and Technology, Islamabad, Pakistan; Surgical Unit 3, Allied Hospital, Faisalabad, Pakistan; and <sup>3</sup>Department of Clinical Pathology, Allied Hospital, Faisalabad, Pakistan

Ubiquicidin (UBI) 29–41 is a cationic, synthetic antimicrobial peptide fragment that binds preferentially with the anionic microbial cell membrane at the site of infection. The current study was conducted to evaluate its potential as an infection-imaging agent in humans. **Methods:** Eighteen patients, 9 female and 9 male (mean age, 31.7 y; range, 5–75 y), with suspected bone, soft-tissue, or prosthesis infections were included in the study.  $^{99m}\text{Tc}$ -UBI 29–41 in a dose of 400  $\mu\text{g}/370$ –400 MBq was injected intravenously in adults. A dynamic study was followed by spot views of the suspected region of infection (target) and a corresponding normal area (nontarget) at 30, 60, 120, and 240 min. The target-to-nontarget ratios were used to find the optimum time for imaging. Whole-body anterior and posterior images were also acquired at 30, 120, and 240 min to study biodistribution. Activity in each organ was expressed as percentage retained dose. Visual score (0–3) was used to categorize studies as positive or negative, with scores of 0 (minimal or no uptake; equivalent to soft tissue) and 1 (mild; less uptake than in liver) being considered negative and scores of 2 (moderate; uptake greater than or equal to that in liver) and 3 (intense; uptake greater than or equal to that in kidneys) being considered positive. Scans were interpreted as true- or false-positive and true- or false-negative on the basis of bacterial culture as the major criterion and the results of clinical tests, radiography, and 3-phase bone scanning as minor criteria. **Results:** The biodistribution study showed a gradual decline in renal activity as percentage of administered dose from 6.53%  $\pm$  0.58% at 30 min to 4.54%  $\pm$  0.57% at 120 min and 3.38%  $\pm$  0.55% at 240 min. The liver showed a similar trend, with values of 5.43%  $\pm$  0.76%, 3.17%  $\pm$  0.25%, and 2.02%  $\pm$  0.30% at 30, 120, and 240 min, respectively. Radioactivity accumulated gradually in the urinary bladder, with values of 4.60%  $\pm$  0.92% at 30 min, 23.00%  $\pm$  2.32% at 120 min, and 38.85%  $\pm$  4.01% at 240 min. Of 18 studies performed with  $^{99m}\text{Tc}$ -UBI 29–41, 14 showed positive findings and 4 showed negative findings. Negative findings were subsequently confirmed to be true negative. The positive findings for 1 scan were interpreted as false positive, as no growth was obtained on bacterial culture and no evidence of

infection was found on minor criteria. In 10 cases, the major criterion was used, whereas in 4 cases minor criteria had to be used for interpretation. Quantitative analysis revealed a maximum mean target-to-nontarget ratio of 2.75  $\pm$  1.69 at 30 min, which decreased to 2.04  $\pm$  1.01 at 120 min. The overall sensitivity, specificity, and accuracy were 100%, 80%, and 94.4%, respectively. No adverse reactions were observed during image acquisition and within 5 d after the study. **Conclusion:**  $^{99m}\text{Tc}$ -UBI 29–41 showed promise in localizing foci of infection, with optimal visualization at 30 min.

**Key Words:** ubiquicidin; antimicrobial peptide; target to nontarget; infection imaging

**J Nucl Med 2005; 46:567–573**

**S**cientigraphic detection of infection has the advantage of whole-body imaging, which might be of great value in cases of occult infection. However, the critical issue is differentiation between infectious and noninfectious inflammatory processes.  $^{67}\text{Ga}$ -Citrate, being the most primitive radio-tracer, has high sensitivity for inflammation but is not specific for infection (1). Labeled leukocytes with  $^{111}\text{In}$ -oxine or  $^{99m}\text{Tc}$ -hexamethylenepropyleneamine oxime are considered the gold standard in nuclear medicine for imaging infection and inflammation (2). However, there are limitations, including use in neutropenic patients, technically difficult and time-consuming procedures with hazard of blood borne infections, such as hepatitis B, hepatitis C, and HIV. Radiolabeled monoclonal antibodies against surface antigens of granulocytes carry a risk of induction of human antimouse antibodies. Similarly, antibody fragments, interleukins, and platelet factor 4 have certain limitations. Cytokines and chemotactic peptides are highly immunogenic and cytotoxic (3). A sensitivity of 85.4% and specificity of 81.7% with  $^{99m}\text{Tc}$ -labeled ciprofloxacin have been reported for infection detection (4). However, emerging antibiotic resistance against such tracers is always a risk (5). False uptake of this labeled antibiotic in sterile inflammation has also been reported (6). Antimicrobial peptides are found in

---

Received Jun. 17, 2004; revision accepted Nov. 17, 2004.  
For correspondence or reprints contact: Muhammad Saeed Akhtar, MBBS, MS, Punjab Institute of Nuclear Medicine (PINUM), P.O. Box 2019, Faisalabad, Pakistan.  
E-mail: Saeed\_pinum@yahoo.com

abundance in mammals, birds, amphibians, insects, and plants, as a part of innate immunity against infection (7). These preferentially bind to a broad spectrum of microorganisms and can be produced by genetically engineered bacteria or by peptide synthesis. The basic interaction between the peptide and the bacteria is based on the cationic (positively charged) domains of the former and the negatively charged surface of the latter (8,9). Ubiquicidin (UBI) 29–41, having amino acid sequence TGRAKRRMQYNRR and a weight of 1,693 Da, is a synthetic antimicrobial peptide fragment that originally was isolated from mouse macrophages (10). This peptide, labeled with technetium, discriminated well between bacterial infection and inflammation induced by lipopolysaccharides of bacterial origin (11). Further evaluation revealed its affinity for *Candida albicans* infections (12). A specific mechanism exists for the bacterial intracellular accumulation of  $^{99m}\text{Tc}$ -UBI 29–41, as it does not concentrate in tumor cells (13). Relatively low affinity has been observed in *Escherichia coli* infection, compared with *Staphylococcus aureus* infection in rabbits; however, the underlying mechanism for this selective accumulation is still not known (14).

Preclinical testing of  $^{99m}\text{Tc}$ -UBI 29–41 in animal models of infection and inflammation showed encouraging results and no side effects. A human biodistribution study by Melendez-Alafort et al. showed rapid clearance of this agent through the kidneys. Approximately 85% of the injected activity was eliminated by renal clearance 24 h after tracer injection. The mean radiation-absorbed dose was 0.13 mGy/MBq for the kidneys, and the effective dose equivalent was  $4.34 \times 10^{-3}$  mSv/MBq. No adverse effects were observed in any subject (15). The current study was a phase I clinical trial of this novel radiopharmaceutical.

## MATERIALS AND METHODS

This pilot study was approved by the local ethical and radiation committee of Allied Hospital and the Punjab Institute of Nuclear Medicine, Faisalabad, and was performed according to provisions of the Declaration of Helsinki regarding medical research involving human subjects.

### Safety of $^{99m}\text{Tc}$ -UBI 29–41

Although animal studies performed with  $^{99m}\text{Tc}$ -UBI 29–41 have shown no adverse reaction and human dosimetry performed by Melendez-Alafort et al. has shown the safety of UBI in humans, toxicity data on human dosage were not available. To investigate dose-related toxicity, we injected 100  $\mu\text{g}/\text{kg}$  of  $^{99m}\text{Tc}$ -UBI 29–41 in 3 rabbits for 3 consecutive days (equivalent to approximately 40 times the maximum predicted human dose). No signs of toxicity were observed 36 h after the last intravenous injection. The animal toxicity study was done in accordance with the current rules of Allied Hospital and Punjab Institute of Nuclear Medicine regarding animal experiments.

### Patient Selection

Eighteen patients with suspected bacterial infection were selected for this study before starting antibiotic treatment. Nine were female and 9 were male (mean age, 31.7 y; range, 5–75 y). No

patient had a history of allergy. Each subject or a parent gave written consent after receiving a full explanation of the procedure.

Patients with suspected bone or soft-tissue infections of the limbs were included in the study. Candidates with suspected infection around a hip prosthesis constituted the rest of this group. Limb lesions were preferred because they could be compared with the healthy contralateral side.

Pregnant or lactating women were excluded from this study. Candidates with known hepatic or renal insufficiency or a history of allergy were also excluded.

### $^{99m}\text{Tc}$ -UBI 29–41 Scintigraphy

**Preparation of  $^{99m}\text{Tc}$ -UBI 29–41.** The Pakistan Institute of Nuclear Science and Technology supplied UBI 29–41 in a freeze-dried kit form. The kit comprised 400  $\mu\text{g}$  of antimicrobial peptide dissolved in 10  $\mu\text{L}$  of a 0.01 mol/L concentration of acetic acid, 10 mg of sodium pyrophosphate, and 2.5 mg of  $\text{SnCl}_2 \cdot 2\text{H}_2\text{O}$ . Each vial was reconstituted with 0.5 mL of saline containing 370–400 MBq (mean  $\pm$  SD,  $376 \pm 11.8$  MBq) of sodium pertechnetate from a freshly eluted  $^{99m}\text{Tc}$  generator (DryTech; Amersham Inc.). The reconstituted vial was shaken for 15 s, followed by incubation at room temperature for 30 min. Afterward, the volume was raised to 1 mL by addition of 0.5 mL of saline. The pH of the solution was in the desired range of 6–7. The entire vial content was taken into a 3-mL syringe and injected intravenously into the patient. For children, the dose was scaled down according to Webster's rule (16).

**Quality Control.** The radiochemical purity of each vial was checked using instant thin-layer chromatography (ITLC-SG strips; Gelman Sciences) and Whatman No. 3 chromatographic strips. Acetone and 85% ethanol were used as solvents. The strips were cut into upper and lower halves and counted for 2 min under a single-head  $\gamma$ -camera (E-Cam; Siemens) equipped with a low-energy all-purpose collimator, using an energy peak centered at 140 keV and a 20% window.

**$^{99m}\text{Tc}$ -UBI Imaging.** The E-Cam, equipped with a low-energy all-purpose collimator, was used for acquisition, and data were processed using the ICON 8.5 Macintosh system (Apple Computer Inc.). Target-to-nontarget ratio (T/NT) was calculated using the region ratio software of the E-Cam.

**Study Protocol.** Baseline investigations of all the subjects, including a complete blood examination (red blood cell count, total lymphocyte count, leukocyte count, erythrocyte sedimentation rate) and urea, creatinine, and liver function tests, were conducted. Urine samples were also collected beforehand for routine chemical and microscopic examination. A dose of 370–400 MBq (10 mCi) of  $^{99m}\text{Tc}$ -UBI 29–41 was given intravenously in 30 s to acquire dynamic images of the suspected area of infection and the corresponding nontarget area. During the study, vital signs were monitored for any significant change from baseline. Blood and urine samples of the patients were checked after 5 d to document any change from prescan values that could be attributed to use of the radiopharmaceutical.

**Imaging Protocol.** The dynamic acquisition comprised 10 frames of 60 s each. Anterior and posterior whole-body images were acquired at 30, 120, and 240 min. Spot views of the region of interest at 30, 60, 120, and 240 min were also acquired, each for 500 kilocounts.

**Biodistribution.** Whole-body images of 3 candidates were used to calculate the biodistribution of  $^{99m}\text{Tc}$ -UBI 29–41. Urine voiding was avoided during the study up to 240 min. A region of interest was drawn around the whole body on anterior and posterior

images, and counts with geometric mean method were considered 100% of the injected dose at that particular time. Similarly, regions of interest were drawn around the liver, kidneys, and urinary bladder, and the percentage injected dose at 30, 120, and 240 min was calculated using the following formula: percentage injected dose in an organ =  $100 \times \text{organ count at particular time} / \text{total-body count at that time}$ . Other subjects were not included in the biodistribution study, as the objective was to have an overview of the behavior of the kit in humans.

### Diagnosis of Infection

Bacterial culture was used as the major criterion to definitively diagnose infection. For patients in whom samples for culturing could not be taken (suspected cases of osteomyelitis and prosthesis infection), minor criteria were defined, including blood complete examination and convincing evidence on radiographs and 3-phase bone scans. Radiographs and 3-phase bone scans were interpreted independently without knowledge of the results of  $^{99m}\text{Tc}$ -UBI 29–41 scanning. Samples for culturing were taken from the infected wound when possible, using a sterile swab or, for closed infections, fine-needle aspiration. The inoculation was on blood agar and MacConkey agar culture media and was followed by incubation at 37°C for 48 h. The microbiologist interpreting bacterial cultures was unaware of the findings of scintigraphy.

### Criteria for Study Interpretation

Images acquired at 30, 60, and 120 min were considered for interpretation. Images obtained at 240 min showed markedly less tracer accumulation than did the initial images and therefore were excluded from the interpretation protocol. The criteria were based on a 4-point visual scale (0–3) in which 0 indicated no or minimal uptake; 1, mild uptake; 2, moderate uptake; and 3, intense uptake, compared with the normal contralateral region. Focal tracer uptake equivalent to kidney activity was considered intense, uptake less

than or equivalent to liver activity was considered moderate, uptake less than liver activity was considered mild, and focal tracer accumulation equivalent to soft-tissue activity was considered minimal or no uptake. A score of 0 or 1 was considered a negative finding, whereas a score of 2 or 3 was considered a positive finding.  $^{99m}\text{Tc}$ -UBI 29–41 findings were finally interpreted as true positive (positive scan findings with cultures positive for bacteria or evidence of infection on minor criteria [complete blood examination, radiography, 3-phase bone scanning]), false positive (positive scan findings with cultures negative for bacteria and no evidence of infection on minor criteria), true negative (negative scan findings with cultures negative for bacteria), or false negative (negative scan findings with cultures positive for bacteria or evidence of infection on minor criteria).

### Quantitative Analysis

Scans with positive findings were analyzed quantitatively by calculating T/NTs for the 30-, 60-, and 120-min images (Fig. 1). Tight placement of the region of interest around the area of increased accumulation of tracer (target) was followed by mirroring of the region over the contralateral site (nontarget).

### Statistical Analysis

Sensitivity, specificity, positive predictive value, negative predictive value, and overall diagnostic accuracy for  $^{99m}\text{Tc}$ -UBI 29–41 scintigraphy were calculated.

## RESULTS

### Safety in Humans

All subjects tolerated intravenous injection of  $^{99m}\text{Tc}$ -UBI 29–41 well. No adverse reactions or significant changes in vital signs were observed in any patient during or after acquisition. The results of follow-up blood and urine exam-

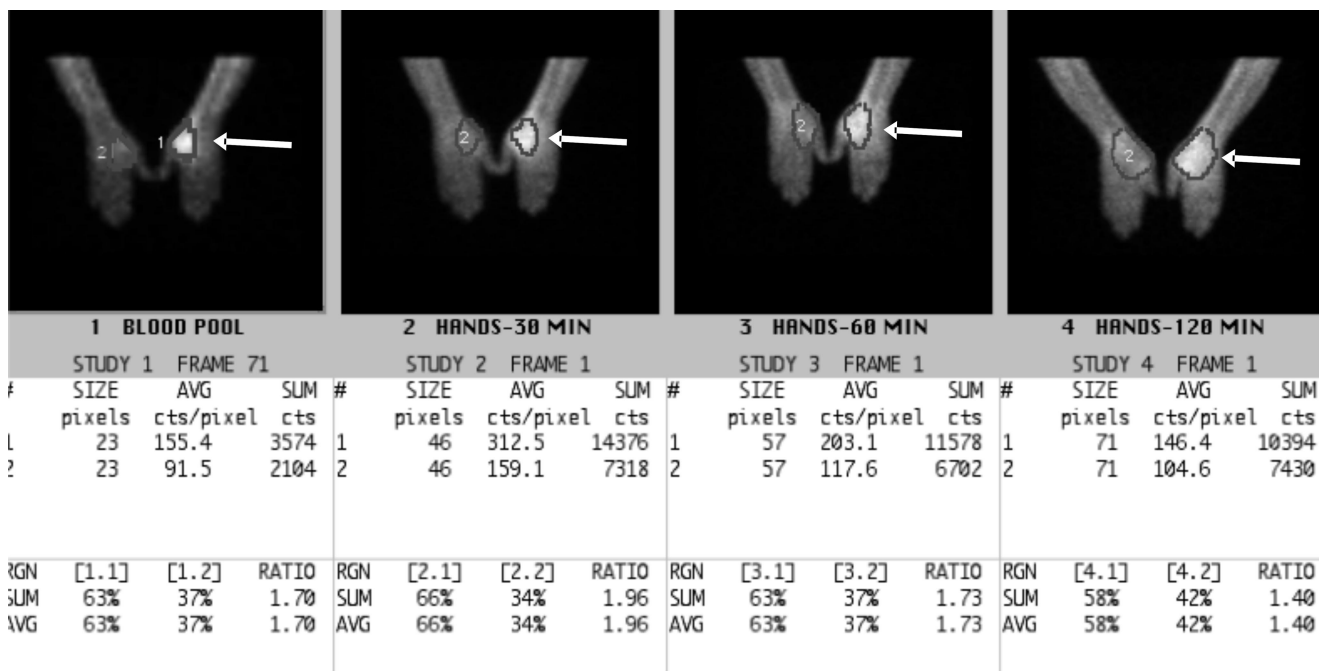
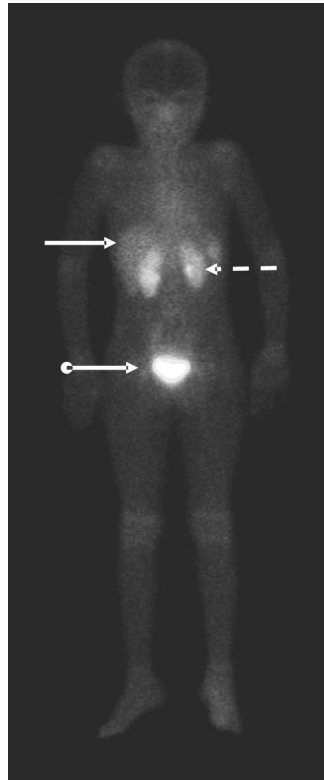
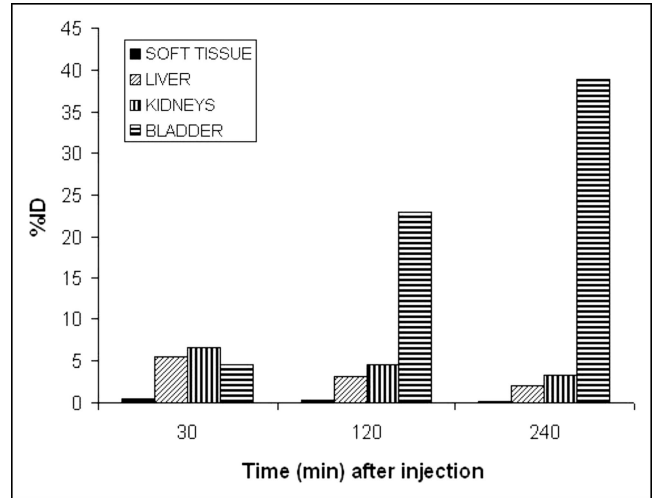


FIGURE 1. Processing page for calculation of T/NT.



**FIGURE 2.** Anterior whole-body image at 30 min after tracer injection showing kidneys (dotted arrow), liver (solid arrow), and urinary bladder (ball arrow).



**FIGURE 3.** Scintigraphic biodistribution of  $^{99m}\text{Tc}$ -UBI 29–41. Percentage injected dose (%ID) data for organs are mean of 3 data points, taking whole-body counts as 100% of injected dose at each interval.

inations matched the baseline test results, except for insignificant changes in the results of the blood complete examination related to the disease process itself. No side effects could be attributed to  $^{99m}\text{Tc}$ -UBI 29–41 during the 5 d after injection.

### Chromatography Results

Radiochemical purity was determined by paper chromatography, which showed >95% labeling efficiency for the  $^{99m}\text{Tc}$ -UBI 29–41 kit. Free technetium remained at <2% until 240 min after reconstitution.

### $^{99m}\text{Tc}$ -UBI 29–41 Studies

Whole-body images of 3 subjects were used for calculating the percentage injected dose in various organs (Fig. 2). The biodistribution data, shown in Table 1 and Figure 3,

revealed gradual excretion of the tracer via the kidneys. Renal activity declined from 6.53%  $\pm$  0.58% of the injected dose at 30 min to 4.54%  $\pm$  0.57% at 120 min and 3.38%  $\pm$  0.55% at 240 min. A similar pattern was observed in liver, with values of 5.43%  $\pm$  0.76%, 3.17%  $\pm$  0.25%, and 2.02%  $\pm$  0.30% at 30, 120, and 240 min, respectively. A rising pattern was noticed in the urinary bladder, with values of 4.60%  $\pm$  0.92% of the injected dose at 30 min, 23.00%  $\pm$  2.32% at 120 min, and 38.85%  $\pm$  4.01% at 240 min.

In studies with positive findings,  $^{99m}\text{Tc}$ -UBI 29–41 scintigraphy showed markedly greater uptake of radiopharmaceutical at the site of infection than on the contralateral healthy side (Fig. 4). Fourteen patients suspected to have infection had positive findings according to the defined criteria. Ten candidates had soft-tissue infections that were confirmed on bacterial culturing, and 3 subjects had bone infections that were interpreted on minor criteria. Cultures were negative for bacteria in 1 patient (patient 6), with no evidence of infection on minor criteria (false positive).

Negative studies showed minimal uptake (score = 1) or no uptake (score = 0) of radiopharmaceutical at the sus-

**TABLE 1**  
Biodistribution Data

Patient no.	%ID in soft tissues			%ID in kidneys			%ID in liver			%ID in urinary bladder		
	30 min	120 min	240 min	30 min	120 min	240 min	30 min	120 min	240 min	30 min	120 min	240 min
1	0.51	0.30	0.24	6.50	4.01	2.89	5.63	2.95	2.08	3.62	21.12	34.45
2	0.47	0.28	0.20	7.15	4.45	3.28	4.59	3.45	1.70	5.40	25.60	39.81
3	0.64	0.36	0.24	5.96	5.15	3.97	6.08	3.12	2.29	4.90	22.23	42.30
Mean $\pm$ SD	0.54 $\pm$ 0.09	0.31 $\pm$ 0.04	0.23 $\pm$ 0.02	6.53 $\pm$ 0.58	4.54 $\pm$ 0.57	3.38 $\pm$ 0.55	5.43 $\pm$ 0.76	3.17 $\pm$ 0.25	2.02 $\pm$ 0.30	4.60 $\pm$ 0.92	23.00 $\pm$ 2.32	38.85 $\pm$ 4.01

%ID = percentage injected dose.



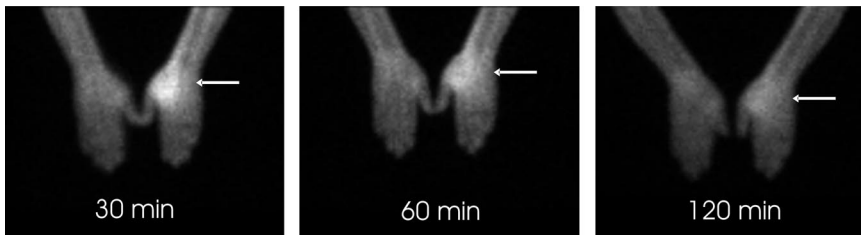


**FIGURE 4.** Positive  $^{99m}\text{Tc}$ -UBI 29–41 scintigraphy findings in patient with infection in medial aspect of right hand. Markedly greater focal tracer accumulation is seen on side with infection (arrows) than on normal contralateral side. Tracer uptake is maximal on image obtained at 30 min.

pected site of infection. All patients in this category ( $n = 4$ ) had negative scintigraphy results (Fig. 5). Three subjects in whom cultures were negative for infection were determined to have soft-tissue swelling (inflammation), and 1 patient in whom minor criteria revealed no evidence of infection was determined to have prosthetic loosening.

For the quantitative analysis, T/NTs were calculated for images acquired at 30, 60, and 120 min to find the optimum time for imaging. The maximum mean T/NT was observed at 30 min after intravenous injection. The T/NTs for all patients at different times are shown in Table 2 and Figure 6.

Among the patients with cultures positive for infection, 56% showed growth of *Staphylococcus aureus*, 33% revealed *Streptococcus pyogenes*, and 11% demonstrated growth of *Pseudomonas aeruginosa*.

Statistical analysis revealed a sensitivity of 100%, whereas specificity was 80% because of 1 false-positive case. Positive predictive value, negative predictive value,

and overall diagnostic accuracy were 92.9%, 100%, and 94.4%, respectively.

## DISCUSSION

Currently available techniques such as ultrasonography, CT, and MRI are anatomically oriented. Despite being highly sensitive and sophisticated, these modalities lack specificity for infection, especially in early phases, when anatomic structures have not yet been altered. Infection and inflammation can be detected early with scintigraphy; however, it is unable to differentiate between infectious and noninfectious inflammation. From the most primitive  $^{67}\text{Ga}$ -citrate imaging to the latest  $^{18}\text{F}$ -FDG PET imaging, the leading question has been unanswered.

Because antimicrobial peptides bind directly to bacteria, these can be considered to be better than pharmaceuticals that have an indirect approach (such as binding to leukocytes or antigranulocyte antibodies). Among the peptides, UBI 29–41 has shown promising results for differentiation between infection and inflammation in animal models (11,12). A freeze-dried kit containing 400  $\mu\text{g}$  of UBI per vial showed encouraging results in animal models, with no adverse effects (14).

A scintigraphic method was used to determine biodistribution so that an overall view of the biokinetics of this kit could be obtained irrespective of attenuation correction, scatter, and physical decay of the nuclide, because the main target was the clinical trial of this peptide. The results revealed gradual excretion of the tracer via the kidneys, with a percentage administered dose of  $6.53\% \pm 0.58\%$  at 30 min and  $3.38\% \pm 0.55\%$  at 240 min. A similar pattern was observed in liver activity. Tracer accumulated gradually in the urinary bladder, with the same parameter values of  $4.60\% \pm 0.92\%$  at 30 min and  $38.85\% \pm 4.01\%$  at 240 min. The percentage administered dose for liver and kidneys was slightly higher than observed by Melendez-Alafort et al. (15), possibly because we did not consider correction parameters. In addition, we injected a higher concentration of peptide (400  $\mu\text{g}$ /patient) than they did (50  $\mu\text{g}$ /patient). They collected urine for estimation of radiotracer excreted by kidneys and observed clearance of 85% of the injected dose after 24 h. The biodistribution pattern in humans observed by Melendez-Alafort et al. and by us in the current study is similar to that observed in animals by Welling et al. (11,12) and Akhtar et al. (14), with only slight differences that could

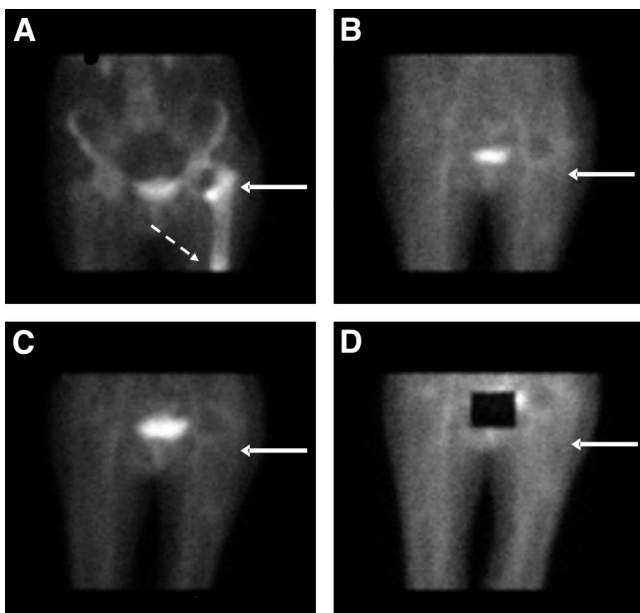


**FIGURE 5.** (A) Focally increased  $^{99m}\text{Tc}$ -MDP uptake during skeletal phase in upper femoral shaft (solid arrow) and tip of hip prosthesis (dotted arrow). (B–D)  $^{99m}\text{Tc}$ -UBI 29–41 scintigrams obtained at 30 min (B), 60 min (C), and 120 min (D) show no tracer uptake to rule out infection at these sites. Urinary bladder is shielded in image obtained at 120 min.

**TABLE 2**  
T/NTs at 30, 60, and 120 Minutes

Patient no.	Type of infection	T/NT			Diagnostic criteria	Visual score
		30 min	60 min	120 min		
1	Soft tissue	1.12	1.05	0.93	Major	1
2	Soft tissue	1.41	1.30	1.30	Major	1
3	Soft tissue	1.34	1.26	1.28	Major	0
4	Chronic osteomyelitis	2.74	2.08	1.85	Minor	3
5	Soft tissue	2.09	1.83	1.79	Major	3
6	Soft tissue	1.61	1.45	1.35	Major	2
7	Soft tissue	2.65	2.38	2.30	Major	3
8	Soft tissue	1.71	1.67	1.76	Major	2
9	Acute osteomyelitis	5.39	4.56	3.99	Minor	3
10	Soft tissue	2.21	1.55	1.56	Major	3
11	Soft tissue	1.70	1.66	1.68	Major	2
12	Acute osteomyelitis	4.21	3.99	2.68	Minor	3
13	Prosthesis loosening	1.26	1.18	1.20	Minor	0
14	Soft tissue	2.12	1.65	1.66	Major	2
15	Soft tissue	5.23	4.32	4.08	Major	3
16	Soft tissue	1.51	1.49	1.50	Major	2
17	Soft tissue	1.96	1.74	1.60	Major	2
18	Soft tissue	6.03	3.97	2.50	Major	3
Mean $\pm$ SD		2.75 $\pm$ 1.69	2.30 $\pm$ 1.30	2.04 $\pm$ 1.01		

have been due to different pharmacokinetics of the peptide and protein binding.

The current study showed that tracer accumulation at the site of infection maximized at 30 min after intravenous injection. T/NTs were  $2.75 \pm 1.69$ ,  $2.30 \pm 1.30$ , and  $2.04 \pm 1.01$  on 30-, 60-, 120-min images, respectively. The spectrum of T/NTs could be due to differences in type and severity of infection in different patients, as explained by the work of Welling et al. (12) and Akhtar et al. (14), who found different T/NTs for different types of bacterial infection. Melendez-Alafort et al. have reported a maximum mean T/NT of  $2.18 \pm 0.74$  at 120 min after tracer injection; however, the types of bacteria detected were not mentioned. The time for maximum T/NT observed in animal studies

was 60 min (11,12,14), but in the current study a somewhat different pattern was observed, 30 min being the time of maximum T/NT, followed by gradual decline. A possible reason for this early maximum tracer accumulation may be subsequent bacterial killing by the antimicrobial peptide, followed by clearance from circulation. The possibility that bacterial killing and subsequent removal from the infection site is the basis for the decreasing T/NT is partly supported by a recent study of Nibbering et al. (17), who used human lactoferrin in doses of 0–40  $\mu\text{g}/\text{kg}$  to treat mice infected with antibiotic resistant *S. aureus* and found a decreased number of bacteria both by tracer accumulation and microbiologically.

According to the visual score, 14 patients had positive findings on scans and 4 had negative findings. Of the patients with negative findings, 3 had soft-tissue swelling and 1 had prosthetic loosening. Cultures were negative for infection in 3 patients with soft-tissue swelling, and minor criteria were used to interpret the case of prosthetic loosening as true negative. Among the 14 patients with positive scan findings, 3 had osteomyelitis interpreted on minor criteria. Ten candidates with soft-tissue disease had cultures positive for bacteria; 56% showed growth of *S. aureus*, 33% revealed *S. pyogenes*, and 11% showed growth of *P. aeruginosa*. However, cultures were negative for bacteria in 1 patient (patient 6), with a visual score of 2 for the scan. Multiple factors may have contributed to this result, including a major study limitation of not using a full range of culture media for growth of anaerobic bacteria, mycobacterium, and fungi. Because of this false-positive case, the specificity of our study dropped to 80%. The only previous human study with this peptide, by Melendez-Alafort et al. (15), showed 100% sensitivity and specificity, but only 6

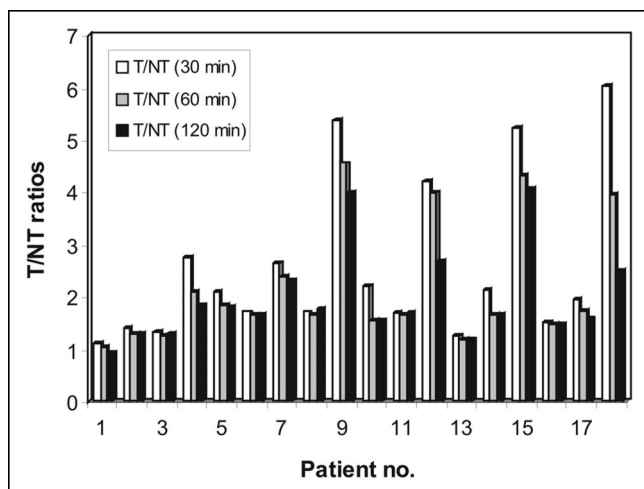


**FIGURE 6.** T/NTs at different intervals in 18 patients examined with infection imaging.

patients were enrolled to investigate the biokinetics of the peptide, and bacterial cultures were available for only 50% of the patients.

The sensitivity, specificity, and overall diagnostic accuracy of  $^{99m}\text{Tc}$ -UBI 29–41 in the current study for infection localization were 100%, 80%, and 94.4%, respectively. Positive and negative predictive values were 92.9% and 100%, respectively.

No adverse reaction was observed during study acquisition and 5 d of follow-up.  $^{99m}\text{Tc}$ -UBI 29–41 scintigraphy is free from the hazards of handling blood products—the major disadvantage of labeled leukocytes. Other advantages include its applicability to leukopenic patients and low probability of resistance to antimicrobial peptides.

## CONCLUSION

$^{99m}\text{Tc}$ -UBI 29–41 is a highly sensitive and specific agent for localizing infective foci in bone and soft tissues of humans. The optimum imaging time for delineation between infectious and inflammatory process is 30 min after intravenous administration of radiotracer.

## ACKNOWLEDGMENTS

This study was supported in part by grant CRP-11263 from the International Atomic Energy Agency. We thank the staff of the Punjab Institute of Nuclear Medicine, particularly Muhammad Yousuf and Athar Hussain Khan; the staff of the Isotope Production Division of the Pakistan Institute of Nuclear Science and Technology; the staff of the Department of Clinical Pathology of Allied Hospital, which provided bacterial culture facilities; and Professor Dr. Riaz Hussain, head of Surgical Unit 3 of Allied Hospital, who assisted with patient selection.

## REFERENCES

1. Palestro CJ. The current role of gallium imaging in infection. *Semin Nucl Med.* 1994;24:128–141.
2. Peters AM. The utility of  $^{99m}\text{Tc}$ -HMPAO leucocytes for imaging infection. *Semin Nucl Med.* 1994;24:110–127.
3. Fischman AJ, Rauh D, Solomon H, et al. In vivo bioactivity and biodistribution of chemotactic peptide analogs in nonhuman primates. *J Nucl Med.* 1993;34:2130–2134.
4. Britten KE, Wareham DW, Das SS, et al. Imaging bacterial infection with  $^{99m}\text{Tc}$ -ciprofloxacin (Infecton). *J Clin Pathol.* 2002;11:817–823.
5. Limoncu MH, Ermertcan S, Cetin CB, Cosar G, Dinc G. Emergence of phenotypic resistance to ciprofloxacin and levofloxacin in methicillin resistant and methicillin-sensitive staphylococcus aureus strains. *Int J Antimicrob Agents.* 2003;5:420–424.
6. Yapar Z, Kibar M, Yapar AF, Togrul E, Kayaselcuk U, Sarpel Y. The efficacy of technetium-99m-ciprofloxacin (Infecton) imaging in suspected orthopaedic infection: a comparison with sequential bone/gallium imaging. *Eur J Nucl Med.* 2001;28:822–830.
7. Ganz ME, Lehrer RI. Defensins and other endogenous peptide antibiotics of the vertebrates. *J Leukoc Biol.* 1995;58:128–136.
8. Epanand RM, Vogel HJ. Diversity of antimicrobial peptides and their mechanisms of action. *Biochim Biophys Acta.* 1999;1462:11–28.
9. Lupetti A, Nibbering PH, Welling MM, Pauwels EKJ. Radiopharmaceuticals: new antimicrobial agents. *Trends Biotech.* 2003;21:70–73.
10. Hiemstra PS, Van den Barselaar MT, Roest M, et al. Ubiquicidin, a novel murine microbicidal protein in the cytosolic fraction of the activated macrophages. *J Leukocyte Biol.* 1999;66:423–428.
11. Welling MM, Paulusma-Annema A, Balter HS, Pauwels EKJ, Nibbering PH. Technetium-99m labeled antimicrobial peptides discriminate between bacterial infections and sterile inflammations. *Eur J Nucl Med.* 2000;27:292–301.
12. Welling MM, Lupetti A, Balter HS, et al.  $^{99m}\text{Tc}$ -labeled antimicrobial peptides for detection of bacterial and *Candida albicans* infections. *J Nucl Med.* 2001;42:788–794.
13. Ferro-Flores G, Arteaga de Murphy C, Pedraza-Lopez M, et al. In vitro and in vivo assessment of  $^{99m}\text{Tc}$ -UBI specificity for bacteria. *Nucl Med Biol.* 2003;30:597–603.
14. Akhtar MS, Iqbal J, Khan MA, et al.  $^{99m}\text{Tc}$ -Labeled antimicrobial peptide ubiquicidin (29–41) accumulates less in *Escherichia coli* infection than in *Staphylococcus aureus* infection. *J Nucl Med.* 2004;45:849–856.
15. Melendez-Alafort L, Rodriguez-Cortes J, Ferro-Flores G, et al. Biokinetics of  $^{99m}\text{Tc}$ -UBI 29–41 in humans. *Nucl Med Biol.* 2004;31:373–379.
16. Thrall JH, Ziessman HA. *Nuclear Medicine: The Requisites.* 2nd ed. St. Louis, MO: Mosby, Inc.; 2001:60.
17. Nibbering PH, Welling MM, Paulusma-Annema A, Brouwer CPJM, Lupetti A, Pauwels EKJ.  $^{99m}\text{Tc}$ -Labeled UBI 29–41 peptide for monitoring the efficacy of antimicrobial agents in mice infected with *Staphylococcus aureus*. *J Nucl Med.* 2004;45:321–326.